

Universality of nucleon-nucleon short-range correlations: Two-nucleon momentum distributions in few-body systems

M. Alvioli,¹ C. Ciofi degli Atti,² L. P. Kaptari,^{3,*} C. B. Mezzetti,³ H. Morita,⁴ and S. Scopetta³

¹ECT*, European Center for Theoretical Studies in Nuclear Physics and Related Areas, Strada delle Tabarelle 286, I-38123 Villazzano (TN) Italy

²Istituto Nazionale di Fisica Nucleare, Sezione di Perugia Via A. Pascoli, I-06123, Italy

³Department of Physics, University of Perugia and Istituto Nazionale di Fisica Nucleare, Sezione di Perugia Via A. Pascoli, I-06123, Italy

⁴Sapporo Gakuin University, Bunkyo-dai 11, Ebetsu 069-8555, Hokkaido, Japan

(Received 26 October 2011; published 17 February 2012)

Using realistic wave functions, the proton-neutron and proton-proton momentum distributions in ${}^3\text{He}$ and ${}^4\text{He}$ are calculated as a function of the relative, k_{rel} , and center of mass, $K_{\text{c.m.}}$, momenta and the angle between them. For large values of $k_{\text{rel}} \gtrsim 2 \text{ fm}^{-1}$ and small values of $K_{\text{c.m.}} \lesssim 1.0 \text{ fm}^{-1}$, both distributions are angle independent and decrease with increasing $K_{\text{c.m.}}$, with the pn distribution factorizing into the deuteron momentum distribution times a rapidly decreasing function of $K_{\text{c.m.}}$, in agreement with the two-nucleon ($2N$) short-range correlation (SRC) picture. When $K_{\text{c.m.}}$ and k_{rel} are both large, the distributions exhibit a strong angle dependence, which is evidence of three-nucleon ($3N$) SRC. The predicted center of mass and angular dependence of $2N$ and $3N$ SRC should be observable in two-nucleon knock-out processes $A(e, e'pN)X$.

DOI: [10.1103/PhysRevC.85.021001](https://doi.org/10.1103/PhysRevC.85.021001)

PACS number(s): 21.30.Fe, 21.60.-n, 24.10.Cn, 25.30.-c

Realistic many-body calculations (see, e.g., Refs. [1–3]) show that a mean-field approach, though describing very successfully many properties of nuclei, breaks down when the relative distance $r \equiv |\mathbf{r}_1 - \mathbf{r}_2|$ between two generic nucleons “1” and “2” is of the order of $r \lesssim 1.3\text{--}1.5 \text{ fm}$. In this region, nucleon-nucleon (NN) motion exhibits short-range correlations (SRC), arising from the interplay between the short-range repulsion and the intermediate range tensor attraction of the NN potential. As a result of such an interplay, the two-nucleon density distribution strongly deviates from the mean-field distribution in that, whereas the latter has a maximum value at zero separation, the former almost vanishes at $r = 0$, increases sharply with increasing separation, overshoots at $r \gtrsim 1.3\text{--}1.5 \text{ fm}$ the mean-field density, and coincides with it at larger separations. The detailed structure of SRC depends on the spin-isospin state of the NN pair, as well as upon the value of the pair center-of-mass (c.m.) coordinate $\mathbf{R}_{\text{c.m.}} = (\mathbf{r}_1 + \mathbf{r}_2)/2$. The study of SRC represents one of the main challenges of modern nuclear physics, since the detailed theoretical and experimental knowledge of the short-range structure of nuclei could provide decisive answers to long-standing fundamental questions, such as the formation and structure of cold dense nuclear matter, the origin of the EMC effect, and the role of quark-gluon degrees of freedom in nuclei (see, e.g., Ref. [4]). SRC generate high-momentum components, which are lacking in a mean-field approach, and give rise to peculiar configurations of the nuclear wave function in momentum space [5]. In particular, if nucleons “1” and “2” become strongly correlated at short distances, the local configuration (in the nucleus center-of-mass frame) characterized by $\mathbf{k}_2 \simeq -\mathbf{k}_1$,

$\mathbf{K}_{A-2} = \sum_{i=3}^A \mathbf{k}_i \simeq 0$, dominates over the average mean-field configuration $\sum_{i=2}^A \mathbf{k}_i \simeq -\mathbf{k}_1$, which is the configuration when the high-momentum nucleon is balanced by all of the remaining $A - 1$ nucleons. Thus, if a correlated nucleon with momentum \mathbf{k}_1 acquires a momentum \mathbf{q} from an external probe and it is removed from the nucleus and detected with momentum $\mathbf{p} = \mathbf{k}_1 + \mathbf{q}$, the partner nucleon should be emitted with momentum $\mathbf{k}_2 \simeq -\mathbf{k}_1 = \mathbf{q} - \mathbf{p} \equiv \mathbf{p}_{\text{miss}}$. Such a qualitative picture is strictly valid only if the center-of-mass momentum of the correlated pair was zero before nucleon removal and, moreover, if the two correlated nucleons leave the nucleus without interacting between themselves and with the nucleus ($A - 2$). Nonetheless, a proton knock-out experiment with detection of emitted neutrons, ${}^{12}\text{C}(p, \text{ppn})$ [6], found that low-momentum neutrons, $p_n < 0.22 \text{ GeV}/c$, were emitted isotropically but that high-momentum neutrons were emitted opposite to the struck proton’s missing momentum \mathbf{p}_{miss} and were, therefore, interpreted as correlated partners of the struck protons [7]. This experiment, later confirmed using electron probes [8], allowed one to obtain the center-of-mass momentum distribution of the correlated pair, finding a Gaussian distribution as predicted long ago in Ref. [9]. Whereas experiments demonstrating the presence of SRC in nuclei and their basic mechanism have eventually been performed, detailed information through the periodic table of their isospin, angular-momentum, and center-of-mass dependencies is still to come. A partial relevant progress has, however, already been done by demonstrating [3,10], in qualitative agreement with the experimental data on ${}^{12}\text{C}$, that the strong correlations induced by the tensor force lead to large differences in the pp and pn distributions at moderate values of the relative momentum of the pair. Such a result has been confirmed in a recent thorough analysis [11] of the relative (integrated over the variables \mathbf{R} and $\mathbf{K}_{\text{c.m.}}$) two-body densities and momentum distributions and their detailed dependence on

*On leave from the Bogoliubov Lab. Theor. Phys., JINR, 141980 Dubna, Russia, through the program Rientro dei Cervelli of the Italian Ministry of University and Research.

the spin-isospin states. As for the angular and center-of-mass dependencies of SRC, in Refs. [3,10] the focus was on the two-body momentum distributions integrated either over the center of mass or the relative momenta, whereas in Ref. [12] the center-of-mass dependence of the relative momentum distributions of ${}^3\text{He}$ and ${}^4\text{He}$ has been investigated in a particular angular configuration, namely when $\mathbf{K}_{\text{c.m.}}$ and \mathbf{k}_{rel} are parallel. In this Rapid Communication the results of calculations for arbitrary mutual orientations of $\mathbf{K}_{\text{c.m.}}$ and \mathbf{k}_{rel} are presented and several universal features of SRC will be demonstrated. Our calculations were performed with nuclear wave functions [13,14] obtained from the solution of the Schrödinger equation containing realistic NN interactions, namely the AV18 [15] and AV8' [16] interactions. We will compare our results with a preliminary analysis of data on ${}^3\text{He}$ from the CEBAF large acceptance spectrometer (CLAS) collaboration at JLab [17]. The summed-over spin and isospin two-body momentum distributions of a nucleon-nucleon pair is defined as follows:

$$n^{NN}(\mathbf{k}_1, \mathbf{k}_2) = \frac{1}{(2\pi)^6} \int d\mathbf{r}_1 d\mathbf{r}_2 d\mathbf{r}'_1 d\mathbf{r}'_2 e^{i\mathbf{k}_1 \cdot (\mathbf{r}_1 - \mathbf{r}'_1)} \times e^{i\mathbf{k}_2 \cdot (\mathbf{r}_2 - \mathbf{r}'_2)} \rho_{NN}^{(2)}(\mathbf{r}_1, \mathbf{r}_2; \mathbf{r}'_1, \mathbf{r}'_2) \quad (1)$$

with

$$\rho_{NN}^{(2)}(\mathbf{r}_1, \mathbf{r}_2; \mathbf{r}'_1, \mathbf{r}'_2) = \int \psi_o^*(\mathbf{r}_1, \mathbf{r}_2, \mathbf{r}_3, \dots, \mathbf{r}_A) \psi_o(\mathbf{r}'_1, \mathbf{r}'_2, \mathbf{r}_3, \dots, \mathbf{r}_A) \delta \times \left(\sum_{i=1}^A \mathbf{r}_i \right) \prod_{i=3}^A d\mathbf{r}_i \quad (2)$$

being the two-body nondiagonal density matrix. By introducing the two-nucleon relative and center-of-mass coordinates and momenta $\mathbf{r} = \mathbf{r}_1 - \mathbf{r}_2$, $\mathbf{k}_{\text{rel}} = (\mathbf{k}_1 - \mathbf{k}_2)/2$, $\mathbf{R}_{\text{c.m.}} = (\mathbf{r}_1 + \mathbf{r}_2)/2$, and $\mathbf{K}_{\text{c.m.}} = \mathbf{k}_1 + \mathbf{k}_2$, the two-nucleon momentum distribution can be defined as follows:

$$n^{NN}(\mathbf{k}_{\text{rel}}, \mathbf{K}_{\text{c.m.}}) = n^{NN}(k_{\text{rel}}, K_{\text{c.m.}}, \Theta) = \frac{1}{(2\pi)^6} \int d\mathbf{r} d\mathbf{R} d\mathbf{r}' d\mathbf{R}' e^{i\mathbf{K}_{\text{c.m.}} \cdot (\mathbf{R} - \mathbf{R}')} \times e^{i\mathbf{k}_{\text{rel}} \cdot (\mathbf{r} - \mathbf{r}')} \rho_{NN}^{(2)}(\mathbf{r}, \mathbf{R}; \mathbf{r}', \mathbf{R}'), \quad (3)$$

where $|\mathbf{k}_{\text{rel}}| \equiv k_{\text{rel}}$, $|\mathbf{K}_{\text{c.m.}}| \equiv K_{\text{c.m.}}$, and Θ is the angle between \mathbf{k}_{rel} and $\mathbf{K}_{\text{c.m.}}$. In what follows the momentum distributions are normalized to unity. Given the formula above, the momentum distribution integrated over the center-of-mass coordinate, $n_{\text{rel}}^{NN}(k_{\text{rel}})$, and the one integrated over the relative momentum, $n_{\text{c.m.}}^{NN}(K_{\text{c.m.}})$, can be obtained, but a more important property, considered in this Rapid Communication, is the dependence of the two-body momentum distribution on the relative momentum k_{rel} for fixed values of the center-of-mass momentum $K_{\text{c.m.}}$ and the angle Θ . In our calculations we used, for ${}^3\text{He}$, the nuclear wave function obtained within the approach from Ref. [13] and corresponding to the AV18 interaction [15] and, for ${}^4\text{He}$, the wave functions of Ref. [14] corresponding to the AV8' interaction [16]. Before discussing our results, let us stress that the independence of the two-nucleon momentum

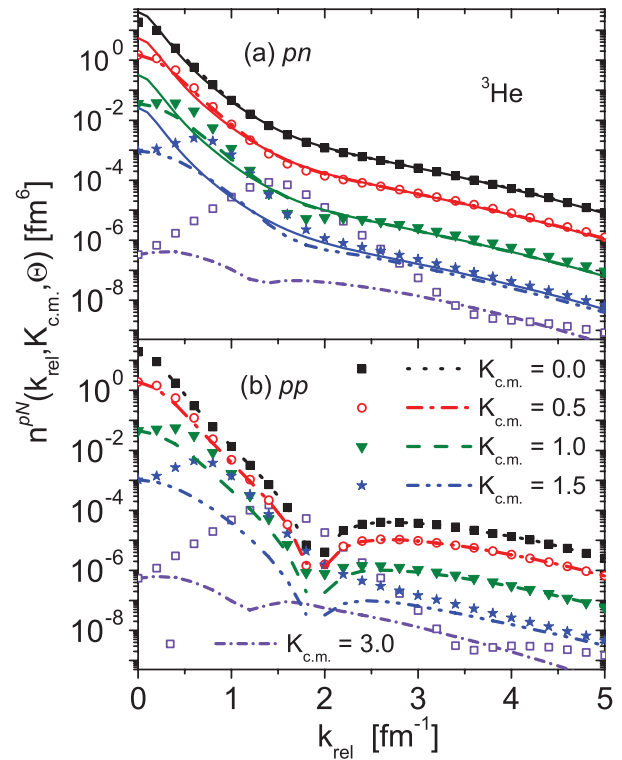


FIG. 1. (Color online) The two-body momentum distributions of pn (a) and pp (b) pairs in ${}^3\text{He}$ normalized to unity, vs. the relative momentum k_{rel} , for fixed values of the center-of-mass momentum $K_{\text{c.m.}}$ and two orientations of them: $\mathbf{k}_{\text{rel}} \parallel \mathbf{K}_{\text{c.m.}}$ (dashed curves) and $\mathbf{k}_{\text{rel}} \perp \mathbf{K}_{\text{c.m.}}$ (symbols). The continuous curves for the pn pair represents the deuteron momentum distribution rescaled by the center-of-mass momentum distribution $n_{\text{c.m.}}^{pn}(K_{\text{c.m.}}) = \int n^{pn}(k_{\text{rel}}, K_{\text{c.m.}}, \Theta) dk_{\text{rel}}$ (see text and Fig. 4). ${}^3\text{He}$ wave function from Ref. [13] and AV18 interaction [15].

distributions on the angle Θ , is evidence of the factorization of the distributions in the variables k_{rel} and $K_{\text{c.m.}}$, i.e., $n^{NN}(k_{\text{rel}}, K_{\text{c.m.}}, \Theta) \simeq n_{\text{rel}}^{NN}(k_{\text{rel}}) n_{\text{c.m.}}^{NN}(K_{\text{c.m.}})$ [18,19].

The pn and pp relative momentum distributions, plotted versus k_{rel} in correspondence with several values of $K_{\text{c.m.}}$, and two angular configurations are shown in Figs. 1 and 2; Fig. 3 shows the ratio for back-to-back nucleons $R^{pn} = n^{pn}(k_{\text{rel}}, K_{\text{c.m.}} = 0)/n_D(k_{\text{rel}})$, whereas the pN center-of-mass momentum distributions $n_{\text{c.m.}}^{pN}(K_{\text{c.m.}}) = \int n^{pN}(k_{\text{rel}}, K_{\text{c.m.}}, \Theta) dk_{\text{rel}}$ are given in Fig. 4; finally, in Fig. 5, the ratio $R_{pp/pn}$ of the correlated pp to pn pairs, extracted from the ${}^3\text{He}(e, e'pp)n$ process [17], is shown. Note that in Figs. 1 and 2 we did not separate the contributions from the various pair spin-isospin states, namely $(ST) = (10), (01)$, L – even, and $(ST) = (11), (00)$, L – odd, where L is the pair orbital momentum. The contribution from the deuteronlike state (10) is shown in Fig. 3, whereas the separate contribution of the four spin-isospin states will be presented in a separate paper [20].

The main features of our results can be summarized as follows: (i) at $K_{\text{c.m.}} = 0$ the results of Ref. [10] are reproduced, namely at small values of k_{rel} the pn and pp momentum distributions do not appreciably differ, with their ratio being closer to the ratio of the pn to pp pairs, whereas at $1.0 \lesssim$

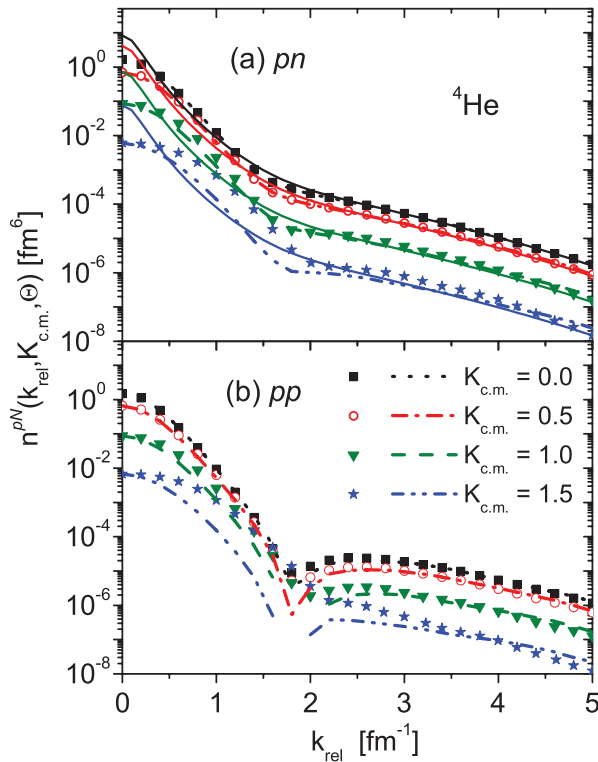


FIG. 2. (Color online) The same as in Fig. 1 but for ${}^4\text{He}$. Correlated variational wave function from [14] and AV8' interaction [16].

$k_{\text{rel}} \lesssim 4.0 \text{ fm}^{-1}$ the dominant role of tensor correlations makes the pn distributions much larger than pp distribution, with the node exhibited by the latter filled up by the D wave in the pn two-body density; (ii) $n^{NN}(k_{\text{rel}}, K_{\text{c.m.}}, \Theta)$, plotted versus k_{rel} , decreases with increasing values of $K_{\text{c.m.}}$; (iii)

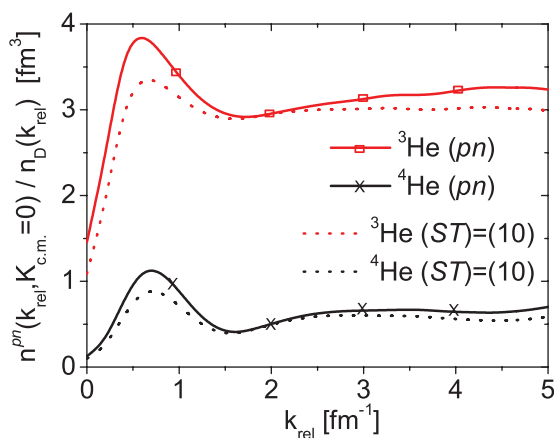


FIG. 3. (Color online) The ratio of the pn momentum distributions $n^{pn}(k_{\text{rel}}, K_{\text{c.m.}} = 0)$ of ${}^3\text{He}$ and ${}^4\text{He}$, shown in Figs. 1 and 2 to the deuteron momentum distribution $n_D(k_{\text{rel}})$ (full lines). The dotted lines represent the contribution from the spin-isospin deuteronlike state $S = 1, T = 0$ in ${}^3\text{He}$ and ${}^4\text{He}$. The different magnitudes of the ratio for the two nuclei is due to the different values of the center-of-mass momentum distribution at $K_{\text{c.m.}} = 0$ (see Fig. 4).

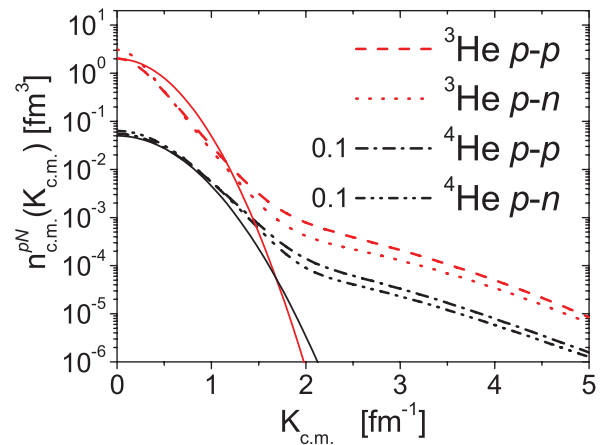


FIG. 4. (Color online) The center-of-mass momentum distribution $n_{\text{c.m.}}^{pn}(K_{\text{c.m.}}) = \int n^{pn}(k_{\text{rel}}, \mathbf{K}_{\text{c.m.}}) d^3k_{\text{rel}}$ for pp and pn pairs in ${}^3\text{He}$ and ${}^4\text{He}$ (reduced by a factor 10). The solid lines correspond to the model of Ref. [9] aimed at describing the low-momentum ($K_{\text{c.m.}} \lesssim 1 \text{ fm}^{-1}$) ($K_{\text{c.m.}} \lesssim 1.0\text{--}1.5 \text{ fm}^{-1}$) part of $n_{\text{c.m.}}^{pn}(K_{\text{c.m.}})$.

starting from a given value of k_{rel} , which for $K_{\text{c.m.}} = 0$ is $k_{\text{rel}} \simeq 1.5 \text{ fm}^{-1}$, and increases with increasing $K_{\text{c.m.}}$, the pn distribution changes its slope and becomes close to the deuteron distribution; (iv) in the region ($k_{\text{rel}} \gtrsim 2 \text{ fm}^{-1}, K_{\text{c.m.}} \lesssim 1 \text{ fm}^{-1}$), n^{NN} becomes Θ independent,¹ which means that $n^{NN}(k_{\text{rel}}, K_{\text{c.m.}}, \Theta) \simeq n_{\text{rel}}^{NN}(k_{\text{rel}})n_{\text{c.m.}}^{NN}(K_{\text{c.m.}})$; for pn pairs, one has $n^{pn}(k_{\text{rel}}, K_{\text{c.m.}}, \Theta) \simeq n_D(k_{\text{rel}})n_{\text{c.m.}}^{pn}(K_{\text{c.m.}})$, where $n_D(k_{\text{rel}})$ is the deuteron momentum distribution and the only A dependence is given by $n_{\text{c.m.}}^{pn}(K_{\text{c.m.}})$; the factorized form for pn pairs describes the $2N$ SRC configuration, when the relative momentum of the pair is much larger than the center-of-mass momentum; (v) at high values of the center-of-mass momentum, of the same order of the (large) relative momentum, more than two particles can be locally correlated, with a resulting strong dependence on the angle and the breaking down of factorization, as clearly shown by Fig. 1 for $K_{\text{c.m.}} = 3 \text{ fm}^{-1}$. According to our preliminary results [20], all of the above remarks appear to hold also for complex nuclei. In particular, the relative momentum distribution, which reflects the local short-range properties of nuclei, exhibits very mild A dependence at $k_{\text{rel}} \gtrsim 1.5\text{--}2.0 \text{ fm}^{-1}$, whereas the center-of-mass momentum distribution at low center-of-mass momenta ($K_{\text{c.m.}} \lesssim 1.0\text{--}1.5 \text{ fm}^{-1}$) can be associated to the mean-field average kinetic energy and approximated by a Gaussian, in agreement with the results of Ref. [9] and the experimental finding for ${}^{12}\text{C}$ of Ref. [6]. Let us now discuss in detail the factorized form of the momentum distributions for pn pairs. To this end we will consider the ratio $R^{pn} = n^{pn}(k_{\text{rel}}, 0)/n_D(k_{\text{rel}})$ and its isospin dependence, presented in Fig. 3, and the center-of-mass momentum distribution $n_{\text{c.m.}}^{pn}(K_{\text{c.m.}})$, presented in Fig. 4. These two figures tell us, first, that the constant value exhibited by the $S = 1, T = 0$ ratio at $k_{\text{rel}} \gtrsim 1.5 \text{ fm}^{-1}$ is unquestionable evidence that in this region the dependence on k_{rel} of the two-body momentum distribution $n^{pn}(k_{\text{rel}}, 0)$ is the same as

¹Such an independence has been checked in a wide range of angles.

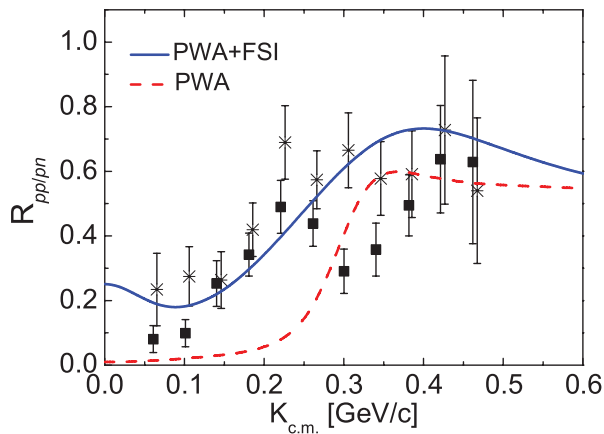


FIG. 5. (Color online) The ratio of the spectator correlated pp and pn nucleon pairs extracted from the ${}^3\text{He}(e, e'pp)n$ reaction and integrated over the pair relative momentum in the range $1.5 < k_{\text{rel}} < 3.0 \text{ fm}^{-1}$ and the angle Θ between $\mathbf{K}_{\text{c.m.}}$ and \mathbf{k}_{rel} [17]. The dashed curve represents the ratio of our theoretical momentum distributions and the full curve also includes the final-state interaction in the spectator pp and pn pairs, calculated by the exact solution of the continuum Schroedinger equation with AV18 potential.

the deuteron one; second, they also tell us that the difference between the ratios for ${}^3\text{He}$ and ${}^4\text{He}$ in the region $k_{\text{rel}} \gtrsim 1.5 \text{ fm}^{-1}$ equals exactly the difference between the values of the center-of-mass momentum distributions at $K_{\text{c.m.}} = 0$, shown in Fig. 4. As a consequence, if we divide the dotted lines by the corresponding values of $n_{\text{c.m.}}^{pn}(0)$, we obtain 1 for both nuclei. Concerning the different behavior of $n_{\text{c.m.}}^{pn}(K_{\text{c.m.}})$ for ${}^3\text{He}$ and ${}^4\text{He}$ at $K_{\text{c.m.}} \lesssim 1.5 \text{ fm}^{-1}$, this is due to the different binding associated with the center-of-mass motion: In ${}^3\text{He}$ the third uncorrelated particle is weakly bound, with a long asymptotic tail, resulting in a sharp peak at $K_{\text{c.m.}} = 0$; thus, the more rapid fall off of the center-of-mass momentum distributions of ${}^3\text{He}$ leads, with respect to the ${}^4\text{He}$ case, to the wider separation of the curves corresponding to various values of $K_{\text{c.m.}}$ presented in Fig. 1. In ${}^4\text{He}$, the overall average density can already be described by a mean-field approach, so the realistic calculation leads, as shown in Fig. 4, to a result

which is practically the same as the one obtained in Ref. [9] within a model based on the mean value of the kinetic energy in a shell-model picture. As for the experimental ratio presented in Fig. 5, it should be pointed out that, whereas this quantity represents a nice confirmation of the dominance of tensor correlations, it cannot provide information about the increase or decrease of the two-body momentum distributions with the increase of the center-of-mass momentum, since the pp and pn distributions may both increase or decrease at the same time, leaving the ratio almost unchanged. A discriminating quantity would be the ratio of pn (or pp) pairs in correspondence of two values of the center-of-mass momentum. As a matter of fact, it can be seen from Fig. 1 that such a ratio at, e.g., $K_{\text{c.m.}} = 0$ and $K_{\text{c.m.}} = 1.5 \text{ fm}^{-1}$, is predicted to be a large positive number.

To sum up, a clear physical picture of the motion of a pair of nucleons embedded in the nuclear medium arises from our calculations. In the region $2 \lesssim k_{\text{rel}} \lesssim 5 \text{ fm}^{-1}$, $K_{\text{c.m.}} \lesssim 1 \text{ fm}^{-1}$, the motion of NN pairs is governed by 2N SRC, characterized by a decoupling of the center of mass and relative motions; for a pn pair, the latter is described by the deuteron momentum distribution and the former is governed by the average mean-field motion. Some aspects of this picture have already been experimentally confirmed [8], whereas some others, e.g., the center-of-mass dependence of two-nucleon momentum distributions, need proper experimental investigations. This picture of a locally correlated pair, with the relative motion being practically A independent, with the A dependence given only by the center-of-mass motion, would be of great usefulness in various fields where SRC have been recently shown to play an important role, such as high-energy hadron-nucleus [21] and nucleus-nucleus scattering [22], deep inelastic scattering [23], the equation of state of nuclear [24], and neutron [4] matters.

H.M. and L.P.K. thanks INFN, Sezione di Perugia, for kind hospitality. The Work of M.A. is supported by the project HadronPhysics2 of the European Commission, Grant No. 227431. Calculations were performed at CASPUR, thanks to the Standard HPC Grants No. 2010 SRCNuc and No. 2011 SRCNuc2.

[1] S. C. Pieper and R. B. Wiringa, *Annu. Rev. Nucl. Part. Sci.* **51**, 53 (2001).
 [2] R. Roth, T. Neff, and H. Feldmeier, *Prog. Part. Nucl. Phys.* **65**, 50 (2010).
 [3] M. Alvioli, C. Ciofi degli Atti, H. Morita, *Phys. Rev. Lett.* **100**, 162503 (2008).
 [4] L. Frankfurt, M. Sargsian, and M. Strikman, *Int. J. Mod. Phys. A* **23**, 2991 (2008).
 [5] L. L. Frankfurt and M. I. Strikman, *Phys. Rep.* **160**, 235 (1988).
 [6] A. Tang, J. W. Watson, J. Aclander, J. Alster, G. Asryan, Y. Averichev, D. Barton, V. Baturin, N. Bukhtoyarova, A. Carroll, S. Gushue, S. Heppelmann, A. Leksanov, Y. Makdisi, A. Malki, E. Minina, I. Navon, H. Nicholson, A. Ogawa, Yu. Panebratsev, E. Piasetzky, A. Schetkovsky, S. Shimanskiy, and D. Zhalov, *Phys. Rev. Lett.* **90**, 042301 (2003).

[7] E. Piasetzky, M. Sargsian, L. Frankfurt, M. Strikman, and J. W. Watson, *Phys. Rev. Lett.* **97**, 162504 (2006).
 [8] R. Subedi, R. Shneor, P. Monaghan, B. D. Anderson, K. Aniol, J. Annand, J. Arrington, H. Benaoum, F. Benmokhtar, W. Boeglin, J.-P. Chen, S. Choi, E. Cisbani, B. Craver, S. Frullani, F. Garibaldi, S. Gilad, R. Gilman, O. Glamazdin, J.-O. Hansen, D. W. Higinbotham, T. Holmstrom, H. Ibrahim, R. Igarashi, C. W. de Jager, E. Jans, X. Jiang, L. J. Kaufman, A. Kelleher, A. Kolarkar, G. Kumbartzki, J. J. LeRose, R. Lindgren, N. Liyanage, D. J. Margaziotis, P. Markowitz, S. Marrone, M. Mazouz, D. Meekins, R. Michaels, B. Moffit, C. F. Perdrisat, E. Piasetzky, M. Potokar, V. Punjabi, Y. Qiang, J. Reinhold, G. Ron, G. Rosner, A. Saha, B. Sawatzky, A. Shahinyan, S. Širca, K. Slifer, P. Solvignon, V. Sulkosky, G. M. Urciuoli, E. Voutier,

- J. W. Watson, L. B. Weinstein, B. Wojtsekhowski, S. Wood, X.-C. Zheng, and L. Zhu, *Science* **320**, 1476 (2008).
- [9] C. Ciofi degli Atti and S. Simula, *Phys. Rev. C* **53**, 1689 (1996).
- [10] R. Schiavilla, R. B. Wiringa, S. C. Pieper, and J. Carlson, *Phys. Rev. Lett.* **98**, 132501 (2007).
- [11] H. Feldmeier, W. Horiuchi, T. Neff, and Y. Suzuki, *Phys. Rev. C* **84**, 054003 (2011).
- [12] R. B. Wiringa, R. Schiavilla, S. C. Pieper, and J. Carlson, *Phys. Rev. C* **78**, 021001(R) (2008).
- [13] A. Kievsky, S. Rosati, and M. Viviani, *Nucl. Phys. A* **551**, 241 (1993) (private communication).
- [14] H. Morita, Y. Akaishi, O. Endo, and H. Tanaka, *Prog. Theor. Phys.* **78**, 1117 (1987).
- [15] R. B. Wiringa, V. G. J. Stoks, and R. Schiavilla, *Phys. Rev. C* **51**, 38 (1995).
- [16] B. S. Pudliner, V. R. Pandharipande, J. Carlson, S. C. Pieper, and R. B. Wiringa, *Phys. Rev. C* **56**, 1720 (1997).
- [17] H. Baghdasaryan *et al.* (CLAS Collaboration), *Phys. Rev. Lett.* **105**, 222501 (2010).
- [18] C. Ciofi degli Atti, L. P. Kaptari, S. Scopetta, and H. Morita, *Few-Body Syst.* **50**, 243 (2011).
- [19] M. Baldo, M. Borromeo, C. Ciofi degli Atti, *Nucl. Phys. A* **604**, 429 (1996).
- [20] M. Alvioli, C. Ciofi degli Atti, L. P. Kaptari, C. B. Mezzetti, and H. Morita (to be published).
- [21] C. Ciofi degli Atti, B. Z. Kopeliovich, C. B. Mezzetti, I. Potashnikova, and I. Schmidt, *Phys. Rev. C* **84**, 025205 (2011).
- [22] M. Alvioli and M. Strikman, *Phys. Rev. C* **83**, 044905 (2011).
- [23] E. Piasetzky, L. B. Weinstein, D. W. Higinbotham, J. Gomez, O. Hena, and R. Shneor, *Nucl. Phys. A* **855**, 245 (2011).
- [24] T. Frick, H. Muther, A. Rios, A. Polls, and A. Ramos, *Phys. Rev. C* **71**, 014313 (2005).